creative commons
COMMONS DEED

저작자표시-비영리-변경금지 2.0 대한민국

이용자는 아래의 조건을 따르는 경우에 한하여 자유롭게

- 이 저작물을 복제, 배포, 전송, 전시, 공연 및 방송할 수 있습니다.

다음과 같은 조건을 따라야 합니다:

저작자표시. 귀하는 원저작자를 표시하여야 합니다.

비영리. 귀하는 이 저작물을 영리 목적으로 이용할 수 없습니다.

변경금지. 귀하는 이 저작물을 개작, 변형 또는 가공할 수 없습니다.

- 귀하는, 이 저작물의 재이용이나 배포의 경우, 이 저작물에 적용된 이용허락조건을 명확하게 나타내어야 합니다.
- 저작권자로부터 별도의 허가를 받으면 이러한 조건들은 적용되지 않습니다.

저작권법에 따른 이용자의 권리는 위의 내용에 의하여 영향을 받지 않습니다.

이것은 이용허락규약(Legal Code)을 이해하기 쉽게 요약한 것입니다.

Disclaimer

dCollection

이학석사학위논문

SHORTROOT 에 의해 조절되는 Quiescent Center 독립적인 뿌리 분열조직 활성조절 유전자 동정

Identification of a novel regulator involved in the Quiescent Center-independent root meristem activity in the SHORTROOT pathway

2015 년 8 월

서울대학교 대학원

생명과학부

김은솔

Abstract

Identification of a novel regulator involved in the Quiescent Center-independent root meristem activity in the SHORTROOT pathway

Eun-Sol Kim

School of Biological Sciences

The Graduate School

Seoul National University

Quiescent center (QC) is known to maintain the root apical meristem (RAM). In the *SHORTROOT* knock-out mutant (*shr*), root growth and QC maintenance are defective. In double knock-out mutants of *SHR* and *PHABULOSA* (*PHB*), root growth is recovered even though QC remains absent. SHR directly regulates the expression of microRNA165/6, which degrades the *PHB* and genes for other class III HD-ZIP transcription factors and establishes their gradient in the stele. In *shr* mutants, PHB exists in a high concentration throughout the stele in the RAM. A high concentration of PHB in *shr* stele suppresses root meristem activity by modulating type B Arabidopsis Response Regulator (B-ARR) activity.

To discover novel factors involved in the SHR-mediated root growth program, we mutagenized *shr-2* mutants with ethane methyl sulfonate (EMS). The lines of which roots grew longer than *shr-2* roots were selected as *shr suppressors of shr* (*ssh*). Among those, we found that *shr ssh206* and *shr ssh80* have mutations in the same gene, *HAWAIIAN SKIRT* (*HWS,* AT3G61590), and followed up for further studies. The root length and meristem size of *shr ssh206* and *shr ssh80* are significantly longer than those of the *shr*. But QC is not recovered completely. Allelism tests revealed that *ssh206* and *ssh80* are different alleles of mutations on the same *HWS* gene. Thus, we designate *shr ssh206* as *shr-2 hws-3,* and *shr ssh80* as *shr-2 hws-4.* *HWS* is expressed in the root cap and in the pericycle of the differentiation zone. Cytokinin marker expression analysis in the *shr-2 hws-3* and *shr-2 hws-4* indicates that the meristem recovery of *shr hws* is not from the recovery of cytokinin signaling. Thus, further research is required to unveil how HWS is involved in the root meristem regulation together with SHR.

Keywords: Quiescent center, Root apical meristem, SHORTROOT (SHR), HAWAIIAN SKIRT (HWS)

Student Number: 2012-20297

CONTENTS

LIST OF FIGURES

Ⅰ. Introduction

1. Root apical meristem (RAM) and growth and development of the root

In plants, organs are postembryonically generated from shoot and root apical meristems (SAM and RAM), while in higher animals, most adult organs are established during embryogenesis (Howell, 1998). It is because plant stem cells are maintained in the SAM and RAM to continuously provide cells that actively proliferate. These divided cells eventually become components of plant organs (Laux, 2003; Weigel and Jurgens, 2002). Therefore, the growth of roots and shoots depends on the maintenance of stem cells and actively dividing cells in the meristem. In this context, studying meristems is a starting point of understanding plant organ development. (Howell, 1998).

In the RAM, four sets of stem cells (stele, cortex/endodermal, epidermal/lateral root cap, and columella initials) surround the quiescent center (QC), thereby establishing a stem cell niche (Dolan et al., 1993) (Fig.1). Stem cells are sources of all the cell types in the root. They continuously undergo asymmetric cell divisions to generate daughter cells: one stays undifferentiated and maintains the stemness and the other serves as an initial for each cell type in the root (Scheres, 2007).

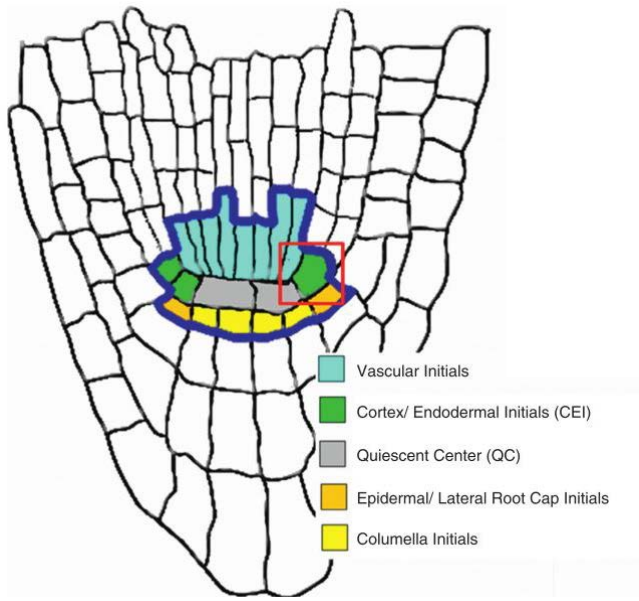

Figure 1. Schematic of a root stem cell niche.

Quiescent center (QC) is surrounded by stem cells. Vascular initials (Blue), Cortex/Endodermal initials (Green), Epidermal/Lateral root cap initials (Orange), and Columella initials (Yellow) divide asymmetrically and provide all the cell types. These are divided into two main pools: proximal and distal stem cells, depending on the position relative to the QC. Vascular initials (Blue), Cortex/Endodermal initials (Green) and Epidermal/Lateral root cap initials (Orange) belong to the proximal stem cells. Columella initials (Yellow) belong to the distal stem cells. The image was adopted from Sozzani *et al.* (2014).

2. Quiescent center (QC) and meristem maintenance

The quiescent center (QC), which is mitotically inactive in comparison to surrounding cells, lies in the center of the stem cells. Laser ablation studies showed that the QC is a source of non-cell autonomous signals that prevent differentiation and maintain the surrounding stem cells (van den Berg et al., 1997).

SHORTROOT (SHR) and SCARECROW (SCR), first identified by their role in radial patterning, are required for QC identity (Di Laurenzio et al., 1996; Helariutta et al., 2000; Sabatini et al., 2003; Wysocka-Diller et al., 2000). *SHR* is transcribed in the stele of both embryonic and post-embryonic roots. SHR protein translated in the stele moves towards QC and endodermis and promotes transcription of *SCR* gene (Nakajima et al., 2001). SCR is cell-autonomously required for QC identity and essential for root meristem maintenance. Therefore, both *shr* and *scr* mutants fail to maintain QC identity (Sabatini et al., 2003).

PLETHORA1 (*PLT1*) and *PLT2* genes are also essential for QC specification and meristem activity (Aida et al., 2004). In *plt1 plt2* double mutant, columella stem cells are not maintained, and decreased root growth and meristem are displayed (Aida et al., 2004).

WUSCHEL-RELATED HOMEOBOX5 (*WOX5*), a homologue of the *WUSCHEL* (*WUS*) gene that maintains stem cells in the shoot meristem (Mayer et al., 1998), is expressed specifically in the QC (Haecker et al., 2004). In *wox5-1* roots, most of QC markers are no longer expressed, consistently the columella stem cells undergo

premature differentiation. Interestingly, the proximal stem cells (Bennett and Scheres, 2010) (Fig. 1) are normal (Sarkar et al., 2007), indicating that *WOX5* is required for the QC identity and for maintaining the distal stem cells (Fig. 1), but not the proximal stem cells, undifferentiated (Bennett and Scheres, 2010; Sarkar et al., 2007). This suggests a possibility that the root growth involves a mechanism independent of the QC.

3. Regulation of QC-independent root meristem activities by PHABULOSA (PHB) and cytokinin

Recently, my group revealed one mechanism regulating root meristem activity in a QC-independent manner (Sebastian et al., 2015). This involves the spatial and dose-dependent regulatory loop between PHABULOSA (PHB) and cytokinin signaling pathways, which acts downstream of SHR.

PHB, one of the HD-ZIP Ⅲ family members, is expressed in the stele. SHR, moving into the QC and endodermis, activates the expression of *miRNA165/6*, together with SCR. *MiRNA165/6* moves out of the endodermis and into the stele, and thereby degrades the mRNAs for HD-ZIP Ⅲ family members. This action was shown to regulate xylem patterning by establishing the gradient of the HD-ZIP Ⅲ family in the stele (Carlsbecker et al., 2010).

shr mutants have defects in root growth and QC maintenance (Koizumi and Gallagher, 2013). While investigating xylem patterning by SHR-miR165/6-HD-ZIP

III's, my group found the recovery of root growth and meristem activity in *shr phb* double mutant without recovery of QC (Sebastian et al., 2015). A further investigation of how PHB suppresses the root meristem activity led to a conclusion that a high concentration of PHB in the stele does this by modulating type B Arabidopsis Response Regulator (B-ARR) activity regardless of presence or absence of the QC (Sebastian et al., 2015).

4. SHORTROOT (SHR) as a master regulator of root development

SHORTROOT (SHR) specifies endodermis layer with SCARECROW (SCR) by promoting asymmetric cell division of cortex/endodermis initial (CEI) (Cui et al., 2007; Nakajima et al., 2001). SHR activates the transcription of *SCR*. This SCR contributes to maintenance of the QC (Sabatini et al., 2003), as mentioned before. SHR also regulates xylem patterning by activating the expression of *miRNA165/6*. From the endodermis, miRNA165/6 moves towards the stele and degrades the mRNAs for HD-ZIP Ⅲ family members. This action establishes the gradient of the *HD-ZIP Ⅲ* family in the stele and thereby the formation of the protoxylem in the stele periphery and the metaxylem in the stele center (Carlsbecker et al., 2010). These findings suggest that SHR is a key regulator of root development in various aspects.

Despite of extensive studies, our understanding of how SHR controls the root stem cell niche and meristem activities together with other regulators is still limited. In this thesis, I aimed to identify a novel gene involved in the QC-independent meristem activities as a part of SHR pathway.

Ⅱ. Materials and Methods

1. Preparation of root growth media and seed sterilization

For one liter of root growth media, 4.33g of Murashige & Skoog Basal salts (Caisson LABS), 0.5g of MES hydrate (Sigma), and 10g of Sucrose (Duchefa Biochemie) were dissolved in triple-distilled water. pH was adjusted from 5.7 to 5.8 with 5M of potassium hydroxide solution. After pH adjustment, 10g of Plant agar (Duchefa Biochemie) was added. Media was autoclaved at 121℃ for 20 minutes. For Basta selection, 8g of Plant agar was added. For Basta selection media, 10mg/ml of glufosinate-ammonium (Fluka) solution and 50mg/ml of carbenicillin solution were prepared by filtering through 0.2μm pore sized filter, and then added to the aforementioned growth media at final concentration of 10μg/ml of glufosinate-ammonium and 50μg/ml of carbenicillin, after cooling down the media to below 60℃.

To sterilize the seeds, sterilization solution was prepared fresh before experiment. For 50ml of sterilization solution, 440mg of sodium dichloroisocyanurate (Aldrich) was dissolved in 5ml of sterilized triple-distilled water, first. Then, 45ml of 95% ethanol was added. Seeds were aliquoted into an Eppendorf tube up to 100 μl. In the laminar flow hood, 1 ml of sterilization solution was added into a tube, mixed well

with seeds, and then incubated for 10 minutes. Sterilization solution was decanted from the tube and 1 ml of 95% ethanol was added. Seeds were mixed well with the ethanol and the ethanol was discarded. This washing step was repeated twice. As a last step, all the ethanol left in the tube was pipetted out. Seeds were left under the laminar flow hood until they were completely dried.

2. Condition of plant growth

Seedlings on the MS media were grown in the temperature-controlled chamber (Hanbaek scientific co.). About 2 weeks later, seedlings were transplanted onto the soil (SunGro) then incubated in the growth room (SEAN). In both cases, temperature was maintained at 22℃ for 16 hours during day time (the time when all lights turned on in the growth chamber or room) and 20℃ for 8 hours during night time (the time when all lights turned out in the growth chamber or room).

3. Screening suppressors of *shr* (*ssh*) by EMS mutagenesis

0.75 g of *shr-2* seeds, approximately 37,500 seeds on the assumption that 50,000 seeds account for one gram, were mutagenized in 40 ml of mutagenesis solution (0.2 v/v % of EMS (Sigma) in 0.1M of phosphate buffer, pH 7.0). In EMS mutagenesis solution, seeds were incubated for 15 hours in room temperature with gentle shaking. Then, seeds were rinsed 20 times with sterilized double-distilled water. After rinsing, the seeds of M0 generations were plated and germinated on the MS media

(composition is described in ‘Preparation of root growth media and seed sterilization’). Root lengths of germinated M1 plants were screened to find possible dominant mutations that suppressed *shr* root phenotype.

After M1 screening, these seedlings were divided into 150 pools, transferred to soil and grown for seed harvesting. After harvesting M2 seeds from M1 pooled plants, 200 seeds from each pool were plated onto MS media and screened for long roots. M2 plants with roots longer more than 1.3 cm were selected and numbered under the name ‘suppressor of *shr* (*ssh*)’. To confirm the phenotype, progeny tests were performed in M3 and M4 generations. *shr ssh* with stable root phenotype was confirmed at M5 generation and *shr ssh206* and *shr ssh80* were selected based on the degree of significance in root growth recovery.

4. Mapping *shr ssh* using Illumina genome sequencing

To identify loci responsible for *ssh206* and *80*, we utilized the genome-data based distribution analysis of single nucleotide polymorphisms (SNPs) between *shr-2* (in Columbia-0 background) and Landsberg *erecta* (L*er*) as shown in recent studies (Austin et al., 2011). Since there was no *shr* mutant in L*er*, we generated *shr* in L*er* ecotype by backcrossing *shr-2* to L*er* four times. Then, each of *shr ssh206* and *shr ssh80* was crossed with *shr-2* in L*er* ecotype and ~200 F2 individuals with long root phenotype were pooled for genomic DNA purification. Whole genome of the pooled mapping population was sequenced at ~50x coverage with Illumina Hi-Seq2000 at

Cornell Genome Center. Illumina genome sequences of each *shr ssh* were compared with the *shr* sequence in sliding window to find SNP frequencies. The regions where SNP against *shr-2* is depleted were identified and the nature of mutations in these regions was further assessed to identify candidate mutations responsible for mutant phenotypes.

5. Root length measurement

Root length were measured with the software ImageJ (www.rsbweb.nih.gov). Picture of seedlings on the growth media were taken and the JPEG image files were opened in ImageJ. Before measurements, the scale was set.

6. Basic fuchsin staining

For basic fuchsin statining, seedlings at 4DAG of each genotype were used. Seedlings were cleared with acidified methanol, in which 10 mL of methanol is added into the solution consisting 2 mL of concentrated HCl (37%) and 38 mL of H_2O. Then seedlings were incubated at 55°–57°C for 15 min. After incubation, the acidified methanol was replaced with basic solution (7% NaOH in 60% ethanol) and seedlings were incubated for 15 min at room temperature. Then rehydration of seedlings took place in several steps. Each time, existed solution was replaced with the ethanol, of which concentration got higher for each step, and incubation carried out for 15 minutes. The concentration of ethanol was first in 40%, then 20%, and

then in 10%. The seedlings were stained for 5 min in 0.01% basic fuchsin solution, and destained in 70% ethanol. Then rehydration was carried out again, with serial increase of ethanol concentration from 40% to 10%. After the last step of rehydration an equal amount of 50% glycerol with the one of existed 10% ethanol was added and incubation carried out for another 30 min. Seedlings were mounted in 50% glycerol.

7. Confocal Laser Scanning microscopy

Confocal images were taken on Carl Zeiss LSM700 confocal microscope with an argon ion laser (488nm excitation, 509nm emission for GFP, 493nm excitation, 636nm emission for PI, and 540nm excitation, 630nm emission for fuchsin). Seedlings were stained with propidium iodide (PI) (Life technologies) to observe cell boundaries. 500X PI stock solution (5mg/ml) was diluted in water before staining. Just before the imaging, seedlings were incubated in PI solution for 2-4 minutes. Seedlings were mounted on the slide glass with water.

8. Cloning *HAWIIAN SKIRT* (*HWS*) gene constructs and *Agrobacterium* transformation

HWAIIAN SKIRT (*HWS*) promoter and coding region were amplified from Col-0 wild-type genomic DNA (Qiagen, DNAeasy Plant Mini kit) by polymerase chain reaction (PCR) using Phusion® High-Fidelity DNA Polymerase (NEW ENGLAND BioLabs) following the manufacturer's instructions. Since *HWS* does not have an

intron, RNA extraction for cDNA cloning was not required. All the constructs were generated by Multisite Gateway® System (Invitrogen), confirmed by restriction enzyme digestion and Sanger sequencing. The dpGreenBarT which is the binary vector with Basta resistant gene were used as a destination vector (Carlsbecker et al., 2010; Lee et al., 2006).

To analyze the expression of *HWS*, *pHWS::erGFP* was generated. To generate the *HWS* promoter and gene, a genomic segment from AT3G61590 was amplified from DNA of Col-0 using the primers HWS F (5'-GGTACATGATTCACACTTTTAC-3') and HWS R (5'-GTTCAAATAAAAGTATCTGGGC-3'). The PCR primers were designed to generate an amplified segment containing 1,291 bp of the promoter region, 419 bp of the 5' UTR, 532 bp of the intron, 1,236 bp of ORF, and 181 bp of 3' UTR as described in the paper by Gonzalez-Carranza et al. (2007). This PCR product was used as templates for amplifying *HWS* promoter and coding region for BP reaction, respectively. *HWS* promoter with attB4 and attB1r sites was amplified using primers pHWS w/ attB4 F (5'-ggggacaactttgtatagaaaagttgGTTTCCAATGCC CATGAAAACG-3') and pHWS w/ attB1r R (5'-ggggactgctttttttgtacaaacttgTCTC AAGAGCCTCTGAAACAAC-3') and then introduced into pDONR P4-P1R vector by BP reaction (In primer sequence, attB sites are in lower case and segment binding sites are in upper case). To generate the *pHWS::erGFP* construct, *HWS* promoter in P4-P1r entry clone, endoplasmic-reticulum targeted GFP (erGFP) in 221 entry clone, and the empty entry clone which has attR2 and attL3 sites were introduced into dpGreenBarT vector by incubating with LR Clonase® II Plus enzyme (Invitrogen).

For *pHWS::gHWS:GFP* construct, *HWS* coding region (gHWS) without stop codon in 221 entry clone was generated. gHWS with attB1F and attB2R sites was amplified using primers gHWS w/ attB1 F (5'-ggggacaagtttgtacaaaaaagcaggctAT GGAAGCAGAAACGTCTTGG-3') and gHWS w/ attB2 R (5'-ggggaccactttgtacaag aaagctgggttAGGAGCAATCTCGAGTCTTGG-3'), and then introduced into pDONR221 vector by BP cloning. *HWS* promoter in P4-P1r entry clone, gHWS in 221 entry clone, and GFP in P2r-P3 entry clone were recombined and introduced into dpGreenBarT destination vector by LR reaction.

For additional complementation tests, *pHWS::gHWS* (with stop codon) and *pHWS::gHWS* (with 3'UTR) constructs were generated. The primers with attB sites to *HWS* gene (with stop codon) and *HWS* 3'UTR were designed. The reverse primer specific to HWS gene with stop codon was designated as gHWS w/ stop and attB (5'-ggggaccactttgtacaagaaagctgggtCTAAGGAGCAATCTCGAGTCT-3'). The primers for *HWS* 3'UTR was designated as HWS 3'UTR w/ attB2r F (5'-ggggacagctttcttgtacaaagtggTTGCAATGAAGAAGCAAATGG-3') and HWS 3'UTR w/ attB3 R (5'-ggggacaactttgtataataaagttgCACCTTCCTTCAATTAATTTC-3'). For entry clone of *HWS* gene with stop codon in pDONR221, *HWS* gene was amplified with primers 'gHWS w/ attB1 F' and 'gHWS w/ stop and attB'. BP reaction with the PCR product and pDONR221 vector generated the construct. *HWS* 3'UTR with attB sites were amplified with the new designated primers (HWS 3'UTR w/ attB2r F and HWS 3'UTR w/ attB3 R) and BP reaction was performed with the pDONR P2R-P3 vector. For *pHWS::gHWS* (with stop codon) construct, *HWS*

promoter in P4-P1r entry clone, *HWS* gene with stop codon in 221 entry clone, empty entry clone which has attR2 and attL3 sites were used. For *pHWS::gHWS* (with 3'UTR) construct, *HWS* promoter in P4-P1r entry clone, *HWS* gene with stop codon in 221 entry clone, and *HWS* 3'UTR in P2r-P3 were used.

To introduce the constructs into the *Arabidopsis* genome, *Agrobacterium* mediated plant transformation was employed. The constructs were transformed into Agrobacterium strain GV3101 with pSOUP by electroporation using Micro-Pulser™ (BIORAD) pulsing 2.2kV for 5mS. Then, the Agrobacterium was incubated in 28℃ shaking incubator for 1 hour in S.O.C media for the recovery. After recovery, transformants were spread on the selection media in which the adequate antibiotics are added (100μl/ml of spectinomycin and 30 μl/ml of gentamicin) and incubated at 28℃ for 48 hours.

9. Plant transformation by floral dipping

Cloned constructs were introduced into *Arabidopsis* genome by floral dipping method (Clough and Bent, 1998). *Agrobacterium* was cultured in 5ml of Luria broth (LB) with selection antibiotics (100μg/ml of spectinomycin and 30 μg/ml of gentamicin) and incubated for 16-20 hours at 30℃ with shaking. *Agrobacterium* was inoculated into 100ml of LB with the antibiotics and incubated for 16-20 hours at 30℃ with shaking. On the day of plant transformation siliques and open flowers

were removed. 100ml of infiltration media was also prepared. 100ml of the infiltration media contains 5g of sucrose, 0.175g of $MgCl_2 \cdot 7H_2O$, and 20.8μl of Silwet L-77 (LEHLE SEEDS). Silwet was added just before the dipping. *Agrobacterium* culture solution was centrifuged at 4800rpm for 12 minutes in 25℃ (HANIL Supra 22k, with A250T-6 rotor). Supernatant was removed and then cells were resuspended with infiltration media (without Silwet). 20.8μl of Silwet was added into resuspended cells and plants were dipped in this media for 5-6 seconds. After dipping, plants were laid in tray letting them not touch each other. Plants were left in the growth chamber for 16-20 hours in the dark with high humidity. The next day, plants were placed upright and grown until their seeds were harvested.

Ⅲ. Results

1. Identification of *suppressor of shortroot* (*ssh*)

To identify candidate genes involved the SHORTROOT (SHR) mediated root growth, we employed a forward genetics approach by searching for mutants suppressing the *shr* root growth phenotype. *shr* insertional null mutant (*shr-2*) in Columbia-0 (Col-0) was mutagenized with ethane methyl sulfonate (EMS) and M2 lines whose roots grew significantly longer than *shr-2* roots were selected as '*shr suppressors of shr-2* (*ssh*)'. Drs. Gustavo Acevedo and Jose Sebastian, the former Lee Lab members at the Boyce Thompson Institute, conducted EMS mutagenesis and screening for *shr ssh.*

From the screening, top 10 candidate suppressors were selected based on the degree of significance in root growth recovery. To identify genes responsible for these suppression, high-throughput genome sequencing based mapping was employed (Huang et al., 2009). More specifically, each of these mutants was crossed with the Landsberg *erecta* (L*er*) into which *shr-2* mutant was integrated by backcrossing for four generations. F2 progenies obtained from the cross between *shr-2* (Ler) and *shr ssh* were screened for long roots and approximately 200 individuals with long root phenotype were pooled for genomic DNA isolation and Illumina sequencing.

Whole genome of the F2 population was sequenced with Illumina Hi-Seq2000 with about 50x coverage of Arabidopsis genome. The sequencing data analysis was carried out by Dr. Linyong Mao in Zhangjun Fei's Lab at the Boyce Thompson Institute. To reveal the candidate genes, distribution of single nucleotide polymorphisms (SNPs) in F2 population was compared with the SNPs of *shr-2* (Col-0 ecotype) as a control (Fig. 2). In the chromosome of mapping population, the locations where mutation occurred come from the Col-0. Therefore, the mutated region responsible for the phenotype will be selected against the genome from L*er*. Thus, the region where the SNP frequencies in comparison to *shr-2* genome sequence are near zero is considered to be close to the mutation responsible for the phenotype. The end of chromosome 4 is where *shr* mutation resides. A large area near the end of chromosome 2 was also suspected as the region for the causal mutation. However, it turned out that all the other candidate mutants also have the SNP depletion in the same area. Thus, we think that this region might have been inverted while the original *shr-2* mutation was generated via fast neutron (Fukaki et al., 1998). Among the *shr ssh* sequence data, we found that both *shr ssh206* and *shr ssh80* have the mutations in the same gene, *HAWAIIAN SKIRT* (*HWS*, AT3G61590). Since *shr ssh206* and *shr ssh80* have mutants on the same gene, these mutants were followed up for a further study.

HAWAIIAN SKIRT (HWS) protein contains an F-box domain and a domain predicted to have ubiquitin-protein transferase activity (Gonzalez-Carranza et al., 2007). In *shr ssh206*, *HWS* gene has C to A mutation on chromosome 3, 22793429

position. This mutation results in a stop codon and shortens the length of HWS protein from 411 amino acids (aa) to 172 aa (Fig. 3). Thus, whole Kelch2 domain cannot be translated and most part of F-box associated interaction domain is truncated (Fig. 4). In *shr ssh80*, G to A mutation on chromosome 3, 22793906 position results in the stop codon (Fig. 3) and shortens the translated region from 411 aa to 331 aa, and thereby a part of Kelch2 domain becomes missing (Fig. 4).

To reassure Illumina sequencing analysis result, we performed Sanger sequencing for each of *shr ssh80* and *shr ssh206*, and confirmed the mutations again.

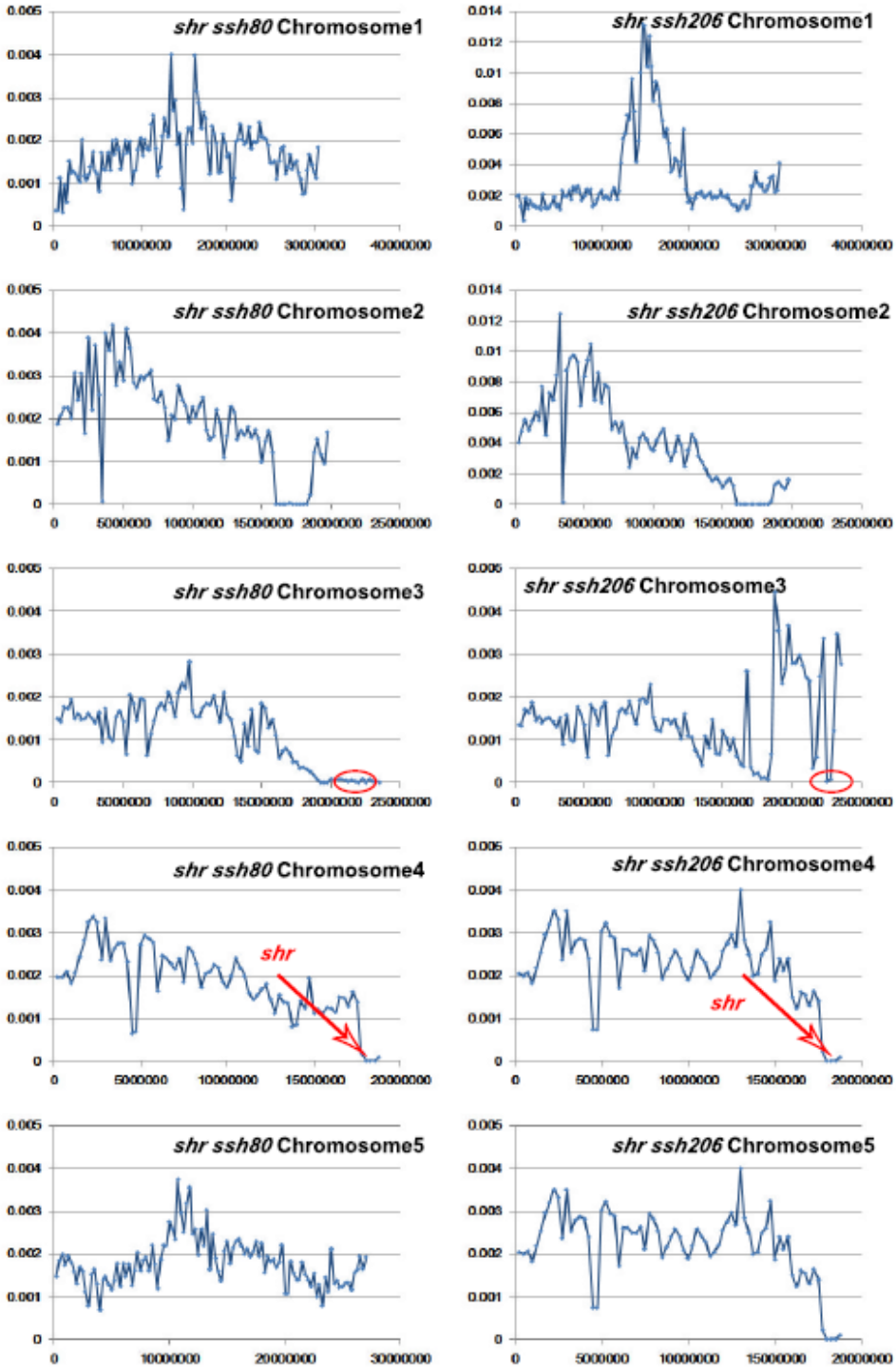
shr ssh80 Chromosome1
shr ssh206 Chromosome1
shr ssh80 Chromosome2
shr ssh206 Chromosome2
shr ssh80 Chromosome3
shr ssh206 Chromosome3
shr ssh80 Chromosome4
shr
shr ssh206 Chromosome4
shr
shr ssh80 Chromosome5
shr ssh206 Chromosome5

Figure 2. SNP distribution of *shr-2 ssh80* and *shr-2 ssh206* in comparison to the *shr-2*.

To reveal the location of mutations responsible for the root phenotype of *shr ssh80* and *shr ssh206*, distributions of SNPs in the genomic DNA from pooled F2's were analyzed in comparison to *shr-2* sequences. The positions where distribution is 0 indicate the potential regions with causal mutation. In both *shr ssh206* and *shr ssh80*, the '0 point' is on the chromosome 3, which is marked with red circle. Arrow indicates the location of *shr*.

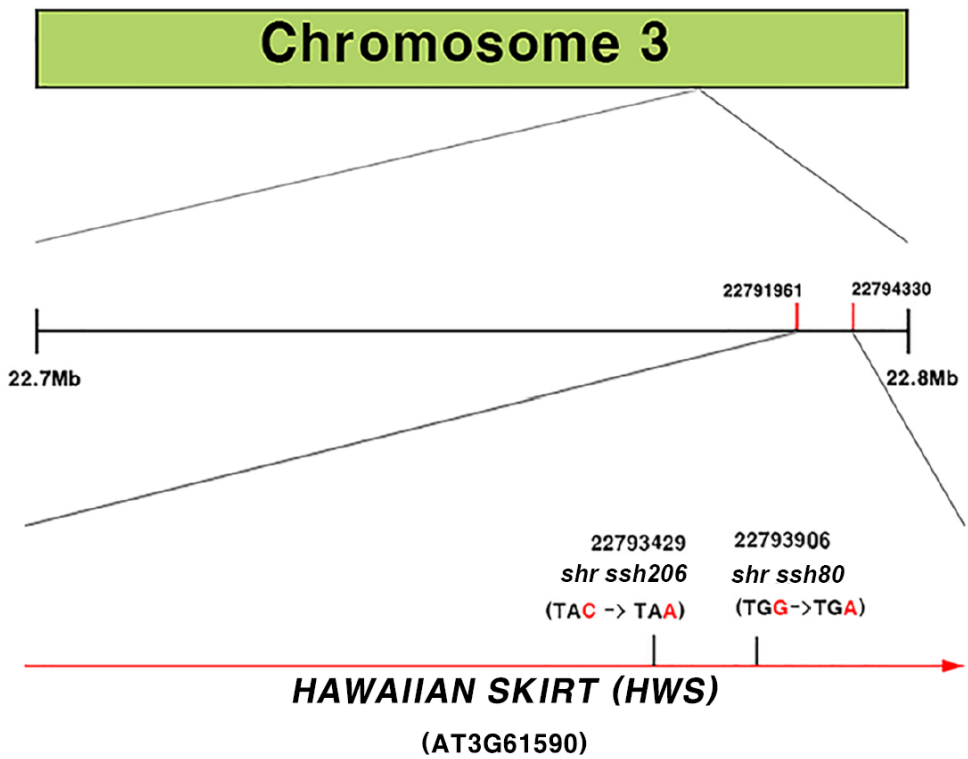

Figure 3. *HAWAIIAN SKIRT* (*HWS*) mutation in *shr ssh206* and *shr ssh80.*

On 22,793,429 position, C to A mutation occurred in *shr ssh206*, which results in TAA stop codon. On 22,793,906 position, G to A mutation occurred in *shr ssh80*. This point mutation generates a stop codon, TGA.

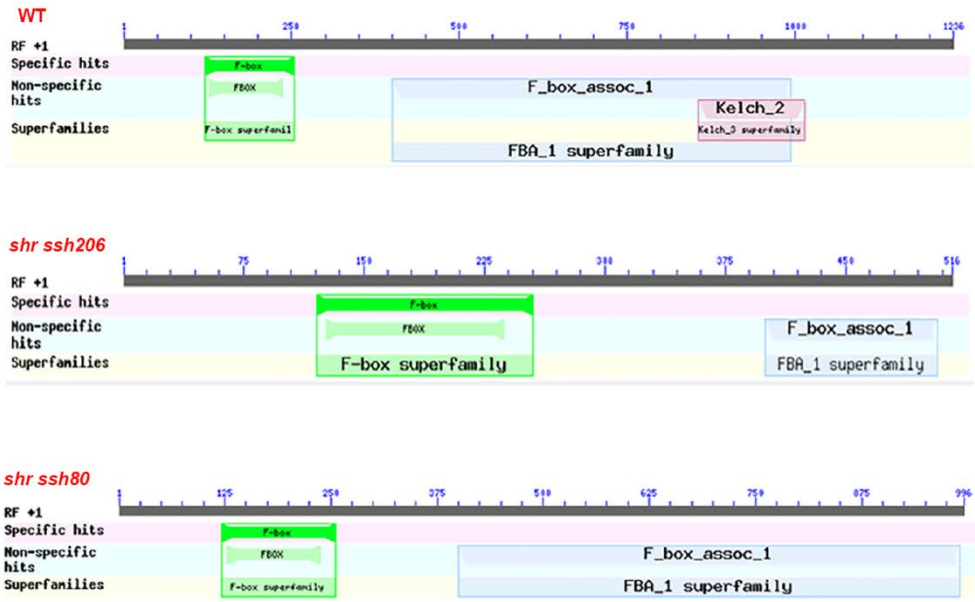

Figure 4. Domains constituting HWS protein and reduction of domains in *shr ssh* mutants. (Results from NCBI BLAST)

HWS protein is composed of F-box domain, F-box associated interaction domain, and Kelch2 domain overlapping C-terminus of F-box associated interaction domain. In *shr ssh206*, the amino acids of HWS protein are shortened from 411 to 172. Therefore whole Kelch2 domain is removed and most of F-box associated interaction domain is truncated. In *shr ssh80*, amino acids are shortened from 411 to 331. Some part of Kelch2 domain is removed.

2. Root phenotype in *shr ssh206* and *shr ssh80* is from the mutations in *HWS*

Our mapping result based on SNP distribution and Sanger sequencing confirmed that *HWS* gene is mutated in *shr ssh206* and *shr ssh80*. To verify that the recovery phenotype came from the *HWS* mutation, three kinds of analyses were proceeded (or are ongoing): 1) phenotypic analysis of *shr hws* double null mutant, 2) allelism test between *shr hws* and *shr ssh206*, between *shr hws* and *shr ssh80*, or between *shr ssh206* and *shr ssh80*, and 3) complementation test to confirm the return of *shr* phenotype when HWS gene constructs (pHWS::gHWS:GFP/ pHWS::gHWS/ pHWS::gHWS with 3'UTR) are introduced into *shr hws*, *shr ssh206*, or *shr ssh80*.

First, we analyzed the phenotype of double null mutant, generated between *shr-2* and *hws-2*. *hws-2* is the T-DNA insertional null mutant (SALK_088349) denominated by Gonzalez-Carranza et al. (2007). The root length of *shr-2 hws-2* (hereafter *shr hws-2*) was significantly longer than the *shr* (Student's t-test; $P < 0.001$, $\alpha = 0.05$) (Fig. 5). This result strongly suggests that the recovery of root length in *shr ssh* comes from the *HWS* mutation.

Second, *shr hws-2* and *shr ssh206*, *shr hws-2* and *shr ssh80*, *shr ssh206* and *shr ssh80* were crossed, respectively, to find if the F1 generation maintains the recovered phenotype, the 'longer root'. In F1's generated from the cross between *shr ssh206* and *shr ssh80*, the root length was measured at 5 Days after germination (DAG). In this paper, 1DAG means the day after cotyledon, not radicle, comes out from seed.

Thus, 0 DAG is the day when cotyledons start to emerge out of the seed coat. Approximately 3 days after placing the media in the growth chamber, cotyledons came out. The root length of F1 generation was significantly longer than the *shr* (Student's t-test; $P < 0.001$, $\alpha = 0.05$) (Fig. 6). This confirms that *ssh206* and *ssh80* are different alleles of the same gene.

In addition, when generating *shr hws-2* double mutant, the F2 progeny of which genotype was heterozygous for *shr* and homozygous for *hws* were crossed with *shr ssh80*. The *shr* and *shr ssh* mutants have the phenotype on the cotyledon and leaf. From 13DAG, the *shr* and *shr ssh* seedlings had yellowish and slightly larger cotyledons than WT. After transplanting these organisms to the soil, their rosette leaves were smaller than the WT. In the F1 generation (*shr/+;hws-2* X *shr ssh80*), the cotyledon phenotypes were divided into a one to one ratio, the WT phenotype to *shr* phenotype. Then, the organisms which have the *shr* cotyledon phenotype developed into F2 progeny. If the mutation in the *shr ssh80* is allele with *HWS*, there will be no progenies which have root phenotype of *shr* mutant. Or if they are not allele, the root phenotype will be divided into a 9:7 (or 9:6:1, depending on the genetic relationships) ratio, the *shr* phenotype versus recovered root phenotype. All of the F2 progenies had recovered root phenotypes, which means that mutated gene in *shr ssh80* that is responsible for the recovered root length is *HWS*. Putting these results together, we conclude that *ssh206* and *ssh80* are another version of *hws*. From now, therefore, the *shr ssh206* will be denominated and designated as *shr hws-3* and *shr ssh80* as *shr hws-4*.

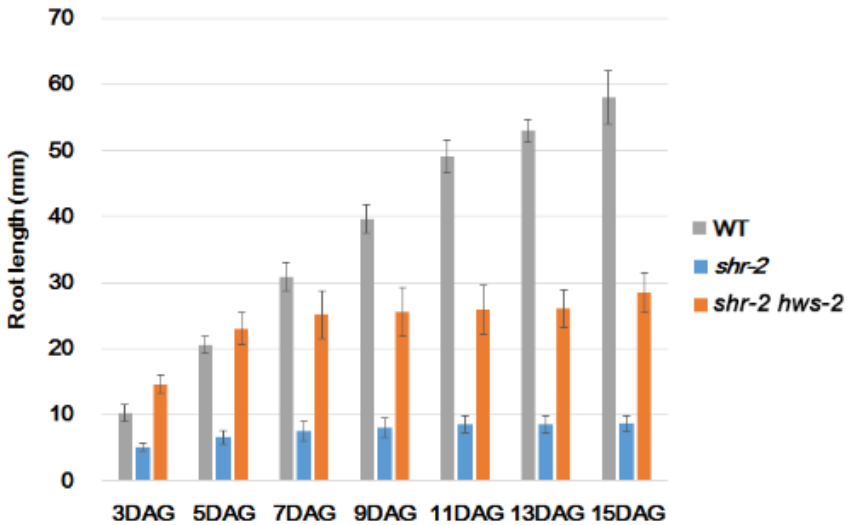

Figure 5. Root growth patterns of *shr-2 hws-2* double knock-out mutants.

The root length of *shr hws-2* was measured every 2 days for 2 weeks with the WT (Col-0), *shr* as a control. The differences in root length between *shr* and *shr hws-2* are significant. Growth of *shr hws-2* slows down at 5DAG. Error bars represent the standard error. (n=10-20 plants)

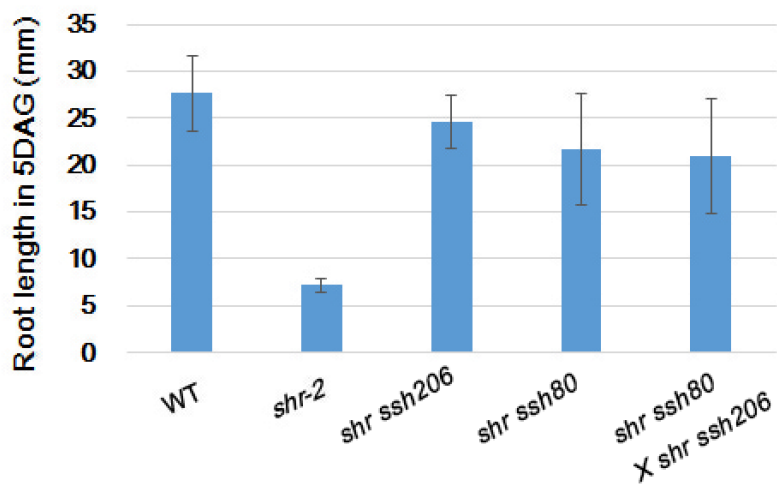

Figure 6. Root length of F1 progenies between *shr ssh206* and *shr ssh80*.

To test whether *ssh206* and *ssh80* are different alleles of the same gene, *shr ssh206* and *shr ssh80* were crossed and the root lengths of F1 progenies were analyzed on 5DAG. The average root length of F1 progenies is significantly longer than the *shr*. Error bars represent the standard error. (n=6-10 plants)

Lastly, for complementation test, 3 kinds of *HWS* gene constructs (*pHWS::gHWS:GFP*/ *pHWS::gHWS*/ *pHWS::gHWS* with 3'UTR) were developed. The HWS translational fusion in which GFP is attached to C-terminus of HWS (*pHWS::gHWS:GFP*) was transformed into *shr hws-3* and *shr hws-4*. To see the location where HWS is expressed and functioning, the transcriptional fusion (*pHWS::erGFP*) and translational fusion (*pHWS::gHWS:GFP*) were transformed into *shr*/+. After selection of transformants by plating T1 seeds on Basta media, the seedlings were transferred into normal MS media. On 5 days after transfer, GFP signal was checked by confocal microscope. By analyzing the *pHWS::erGFP* transgenic WT background mutants, it was determined that *HWS* is expressed in the root cap and the stele (Fig. 13), which is also described in the '6. SHR regulates HWS expression in the stele'. The fact that *HWS* is expressed in the root cap was already checked by Gonzalez-Carranza et al. (2007). In the *pHWS::gHWS:GFP* transgenic mutants, however, there was no GFP signal. We can think of two possibilities why GFP was not expressed. First one is that HWS-GFP might not be able to fold properly as a fusion protein. Second reason might be because HWS is the F-box protein that is recruited to an ubiquitination pathway and to be degraded. With these potential reasons in consideration, we developed another two constructs and transformed them into *shr hws-3* and *shr hws-4*. The cloned constructs were the HWS without GFP (*pHWS::gHWS*) and the *HWS* with 3'UTR (*pHWS::gHWS* with 3'UTR) under *HWS* promoter. If HWS with GFP was misfolded, complementation would occur only in mutants introduced with *pHWS::gHWS* or *pHWS::gHWS* with

3’UTR. If HWS were recruited to the ubiquitination pathway, complementation would occur in all kinds of transformants including the *pHWS::gHWS:GFP* transgenic mutants. Till now, T1 transformants with *pHWS::gHWS:GFP* were selected by Basta resistance and are grown in soil. The transformation of *pHWS::gHWS* and *pHWS::gHWS* with 3’UTR constructs was performed and T0 plants are growing in soil. After collecting the T1 generations, phenotype will be analyzed and *HWS* as *SSH* will be further verified.

3. Meristem defects in the *shr* is recovered in the *shr hws*

To ensure that *shr hws* mutants have recovered the root growth and meristematic activity, phenotype was further analyzed. The roots of *shr hws-2*, *shr hws-3*, and *shr hws-4* were much longer than the *shr* roots (Fig. 7C). To analyze the root growth behavior of *shr hws* mutants in more detail, their root lengths were measured every 2 days for 2 weeks. The wild type (WT) organisms, of which ecotype is Columbia-0 (Col-0), *shr-2*, and *hws-2* mutant were measured together as controls.

Col-0 and *hws* grew continuously until 15DAG. In *shr*, on the other hand, the root growth slowed down at 5DAG. In 3DAG, root length of *shr hws-3* and *shr hws-4* was already much longer than the one of *shr* (Student's t-test; $P < 0.001$, $\alpha = 0.05$) (Fig. 7B). Until 7DAG, *shr hws-3* and *shr hws-4* roots grew actively showing little difference from WT's, but their growth were significantly slowed down after then (Fig. 7A, B).

To analyze the meristem activity further, meristem size of *shr hws-3* and *shr hws-4* was measured and compared with the Col-0 and *shr*. The meristem size is represented by the number of cells in a cortex layer in the meristematic zone (Perilli et al., 2010). The meristem size measured at 5DAG indicated that meristems in the *shr hws-3* and *shr hws-4* are much bigger than the one in *shr* (Student's t-test; $P < 0.001$, $\alpha = 0.05$) (Fig. 8) and similar to the WT. Taken together, the meristem activity of *shr hws* is recovered from the *shr*.

A

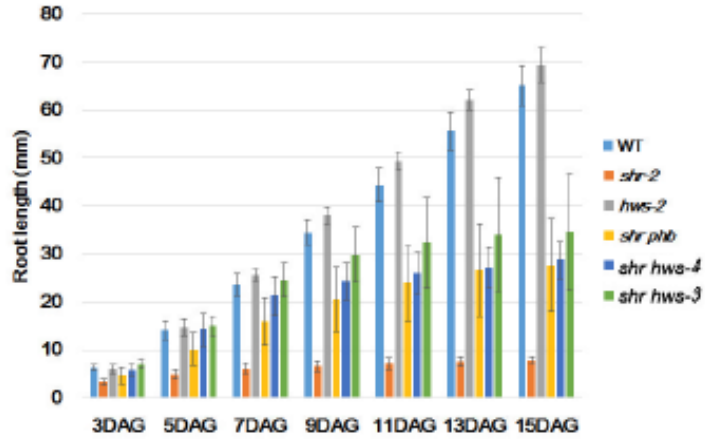
80
70
60
50
40
30
20
10
0
Root length (mm)
3DAG
5DAG
7DAG
9DAG
11DAG
13DAG
15DAG
WT
shr-2
hws-2
shr phb
shr hws-4
shr hws-3

B

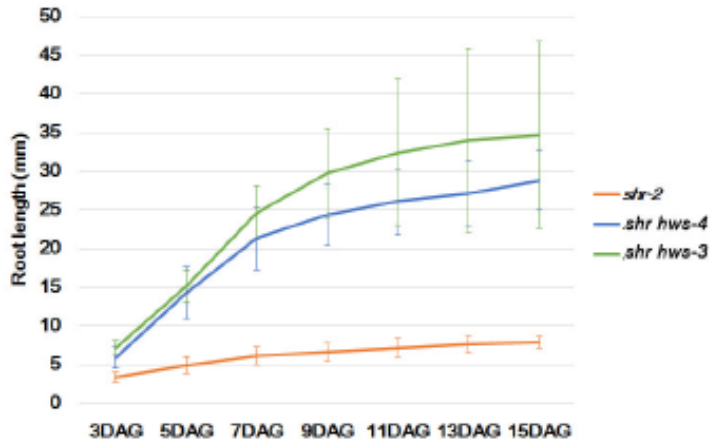
50
45
40
35
30
25
20
15
10
5
0
Root length (mm)
3DAG
5DAG
7DAG
9DAG
11DAG
13DAG
15DAG
shr-2
shr hws-4
shr hws-3

C


WT
shr
shr-2 hws-2
shr-2 hws-3
shr-2 hws-4

Figure 7. Root length phenotype of *shr hws* mutants.

(A) The root growth of *shr hws-3* and *shr hws-4*. The root length was measured every 2 days for 2 weeks with the WT (Col-0), *shr, hws, shrphb* as a control. WT and *hws* grow continuously until 15DAG. While growth of *shr hws-3, shr hws-4,* and *shrphb* slows down on 7DAG, and the growth of *shr* does on 5DAG. Error bars represent the standard error. (n=10-20 plants)

(B) The difference in root growth between *shr* and *shr hws*. Simplified graph from (A). To clarify the differences in root growth, root length of *shr, shr hws-3,* and *shr hws-4* was compared. The differences of root length between *shr* and *shr hws-3* or between *shr* and *shr hws-4* are significant. Error bars represent the standard error. (n=10-20 plants)

(C) Root length phenotype of *shr hws-2, shr hws-3,* and *shr hws-4*. Seedling of each mutant displays significant recovery in root length. Image was taken on 5DAG. Scale bar = 1.5 cm

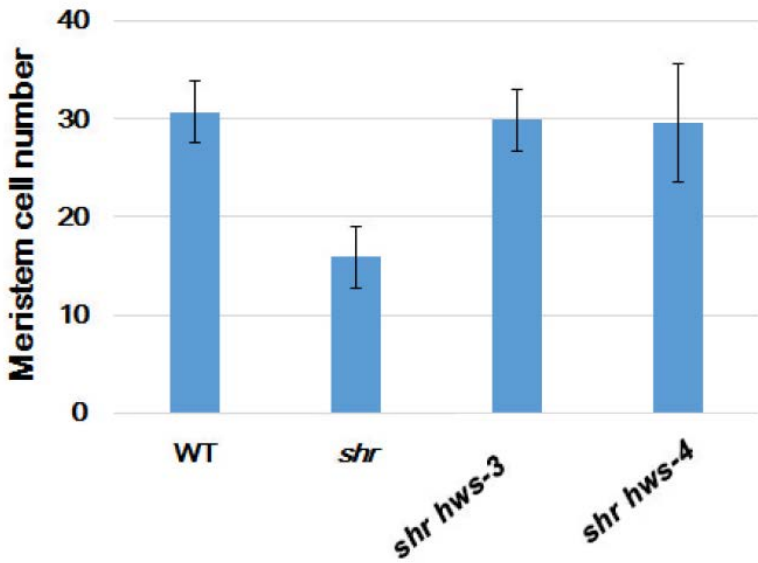

Figure 8. Meristem size of *shr hws.*

The number of isodiametric cells in the cortex layer of *shr hws* was measured at 5DAG. The meristem size of *shr hws-3* and *shr hws-4* is significantly larger than the one of *shr*. Error bars represent the standard error. (n=10 plants)

4. The *shr hws* recovers meristem activity in a QC-independent manner

As mentioned before, SHR and SCR are required for QC identity (Di Laurenzio et al., 1996; Helariutta et al., 2000; Sabatini et al., 2003; Wysocka-Diller et al., 2000). Thus, *shr* mutants have defects in root growth and QC maintenance (Koizumi and Gallagher, 2013). To find whether the recovery of meristem comes from the QC restoration, we observed the structure of meristem of *shr hws*, including QC.

The structure of *shr hws* meristem was observed by confocal microscope at 5DAG (Fig. 9). The *shr* had collapsed QC and the surrounding cell layer, consistent with the former research (Koizumi and Gallagher, 2013). The definite QC structure was not found in *shr hws-3* and *shr hws-4*, which means QC has not recovered completely.

It is possible that *shr hws-3* and *shr hws-4* are hypomorphic mutants since peptides constituting functional domains of HWS are truncated because of the stop codon from the EMS mutagenesis in each *shr hws* mutants. Thus, there were variations in phenotype under one genotype background. The root length was not identical among individuals of *shr hws-3* and *shr hws-4*, still it was much longer than the *shr* mutant root, which was phenotypically and statistically analyzed (Fig. 7). The phenotype of cells located on the QC position was also variable among individuals. Some individuals have collapsed QC, just like *shr*, but some have QC-like cells (Fig. 9).

It was not clear to conclude that the QC remains absent in *shr hws*, because QC-like structures were observed in some individuals. To understand this more clearly,

we introduced the *pWOX5::erGFP* into *shr hws* mutants. *WOX5* is expressed specifically in the QC in the WT background (Haecker et al., 2004). In the *shr* background, *WOX5* expression disappeared at 5DAG (Fig. 10), the time when QC was not maintained (Helariutta et al., 2000; Nakajima et al., 2001). The *shr hws* background seedlings were also investigated in 5DAG. *WOX5* expression was not shown in *shr hws* backgrounds, indicating QC is not recovered from the *shr* (Fig. 10).

Putting these results together, QC is not recovered clearly in both *shr hws* mutants, although the root length is recovered. The meristem cell number of *shr hws* is almost equivalent to that of WT (Fig. 8). This suggests that a critical cause of meristem recovery in *shr hws* is not from the QC maintenance. Therefore, additional research is required to find the mechanism underlying how *shr hws* recovers meristem.

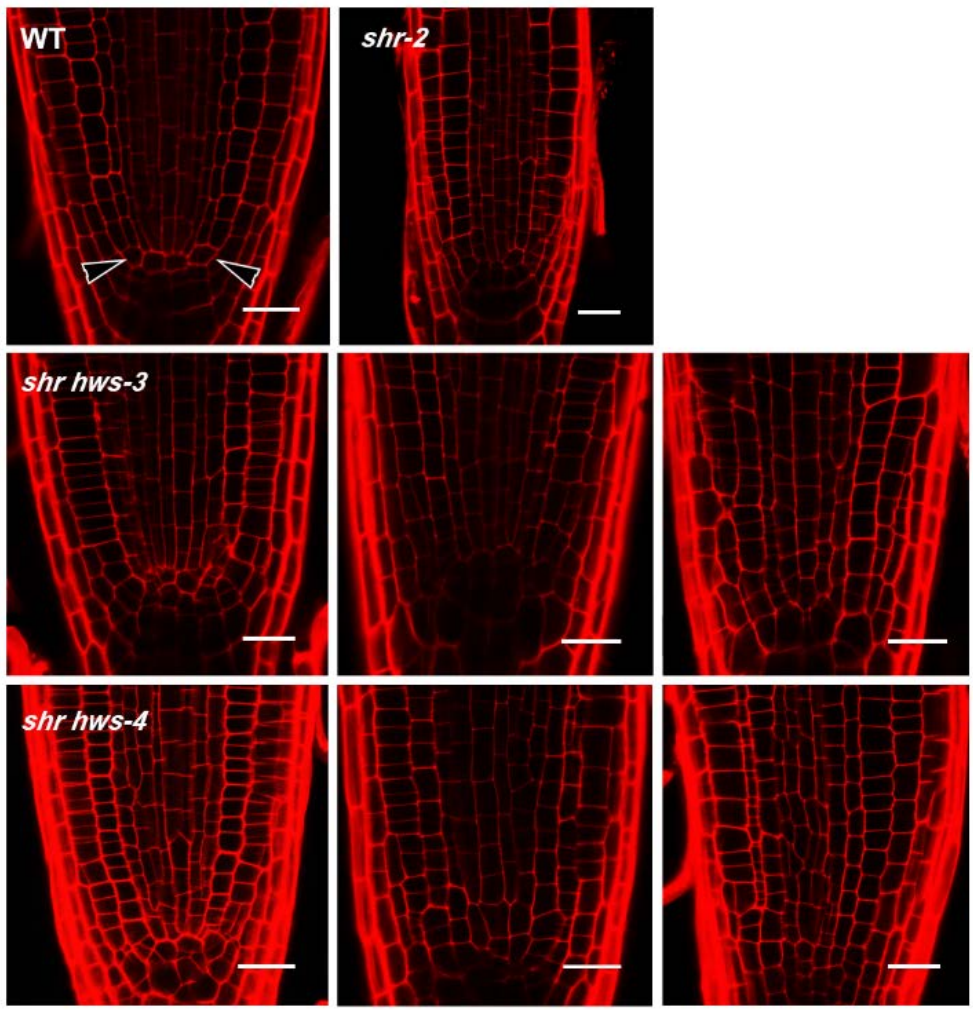

Figure 9. Structure of cells on the QC position in *shr hws*.

The *shr* has collapsed QC and the surrounding cell layer. *shr hws* mutants also have the collapsed QC. But some individuals have imperfect QC that seems to have undergone cell division (Left panel in a second and third row). Black arrowheads indicate the QC. Image was taken at 5DAG. 10 organisms were analyzed for each genotype. Scale bars: 20 μm

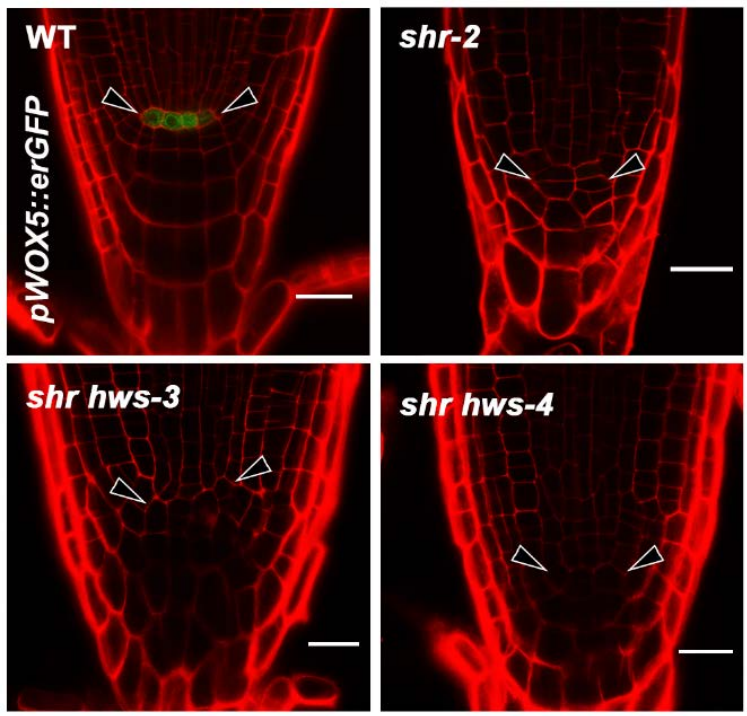

Figure 10. Expression of *WOX5* in *shr hws*.

WOX5 is expressed specifically in the QC in the WT background. In *shr* mutant, *WOX5* expression disappears. The expression of *WOX5* is also disappeared in both *shr hws-3* and *shr hws-4*, indicating that QC is absent and is not recovered from the *shr* phenotype. Black arrowheads indicate the QC (or the sites where QC should be located). Image was taken at 5DAG. 10 to 30 organisms were analyzed for each genotype. Scale bars: 20 μm

5. Cytokinin signaling is not restored in *shr-2 hws-3* and *shr-2 hws-4* mutants

As mentioned before, my group revealed a mechanism regulating root meristem activity in a QC-independent manner in *shr phb* mutant. Root growth defects in *shr* mutants are recovered in *shr phb* double mutant, however, QC remains absent (Fig. 7A) (Sebastian et al., 2015). In *shr* mutants, PHB exists in a high concentration inside the stele. A high concentration of PHB in *shr* stele suppresses root meristem activity by suppressing B-ARR activity in the presence of high cytokinin. Two Component signaling Sensor (TCS) is a synthetic cytokinin reporter construct with B-ARR binding elements (Muller and Sheen, 2008). Thus, TCS expression is absent in the stele of *shr*, but recovered in *shr phb* (Sebastian et al., 2015).

The phenotype of *shr hws-3* and *shr hws-4* that recover meristem activity without complete restoration of QC is very similar to *shr phb*. Thus, we investigated whether *shr hws-3* and *shr hws-4* recover meristem activity via cytokinin signaling like what *shr phb* does, by analyzing expression of cytokinin markers. Two kinds of cytokinin markers were employed, TCS and ARR5. ARR5 (Arabidopsis Response Regulator 5) is a type A cytokinin responsive regulator, which is activated by B-ARRs (Müller and Sheen, 2007; Lohar et al., 2004). TCS expression was analyzed in *shr hws-3* and ARR5 expression was analyzed in both *shr hws-3* and *shr hws-4*. TCS was expressed in the root cap and root stele of the WT. In the *shr* background, TCS expression was absent, however it was restored in the *shr phb*, which is consistent with the report by

Sebastian et al. (2015). Distinct from *shr phb*, TCS expression was not restored in the root stele of *shr hws-3*, and diminished in the root cap (Fig. 11).

ARR5 was expressed in root cap and stele of every backgrounds (WT, *shr-2, shr-2 hws-3,* and *shr-2 hws-4*) at 5DAG. In WT, expression of ARR5 was specific to the procambium (Bishopp et al., 2011). In the *shr-2, shr-2 hws-3,* and *shr-2 hws-4* mutant background, this pattern was collapsed. To confirm the location where ARR5 is expressed, Z- section was performed. The ARR5 was expressed in some part of (not every) procambium and some part of pericycle. There was no significant difference in ARR5 expression pattern between *shr-2* and *shr-2 hws-3* or *shr-2 hws-4* mutants (Fig. 12).

Considering that there may be some temporal regulation in cytokinin signaling, expression pattern of *ARR5* was further analyzed in 8 and 10 DAG. The day performing analysis was determined based on the root growth rate (Fig. 7B). Strikingly, GFP signal was significantly reduced in all the mutants, *shr*, *shr hws-3*, and *shr hws-4* in 8DAG in comparison to the WT. In 10 DAG, the GFP signal faded away in these mutants even though there were some residual signals in the WT (Fig. 12).

Putting these results together, the root meristem recovery of *shr hws-3* and *shr hws-4* is not from the cytokinin signaling. This is distinct from what my lab previously found with *shr phb*. To reveal the recovery mechanism in *shr hws-3* and *shr hws-4*, additional research is required which will be described in ‘Discussion’.

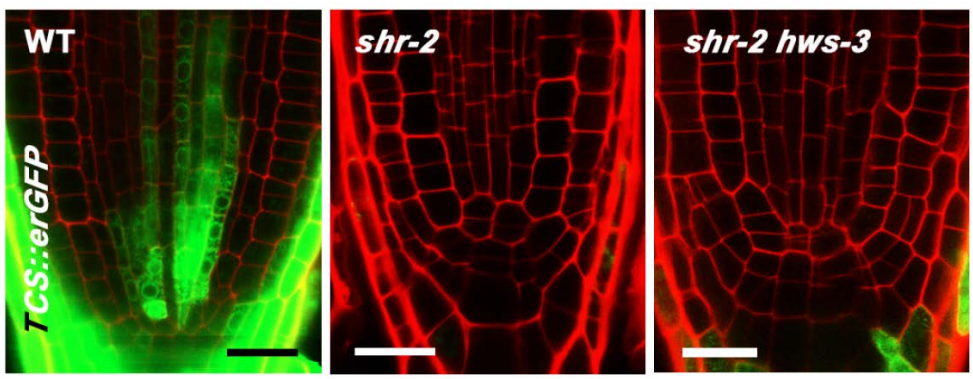

Figure 11. Expression of *TCS::erGFP* in *shr-2 hws-3*.

TCS::erGFP expression in WT, *shr-2*, and *shr-2 hws-3* in 5DAG. GFP is expressed strongly in the root cap and procambium of WT. In *shr-2*, GFP in procambium is not expressed. In the root cap, diminished or absent signal is shown depending on the individuals. There was no significant difference of *TCS::GFP* expression between *shr-2* and *shr-2 hws-3*. 10 organisms were analyzed for each genotype. Scale bars: 20 μm.

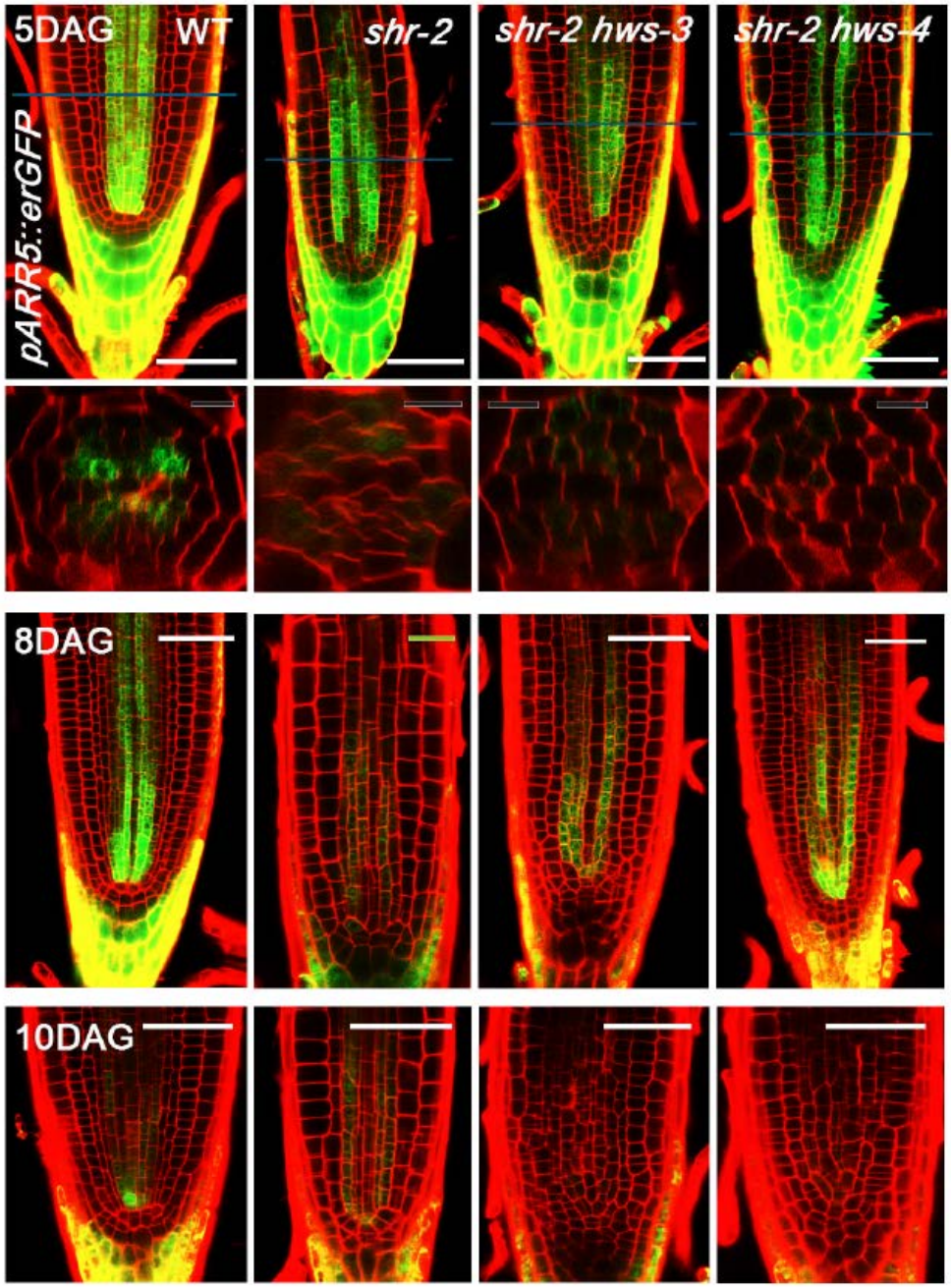
5DAG
WT
shr-2
shr-2 hws-3
shr-2 hws-4
pARR5::erGFP
8DAG
10DAG

Figure 12. Expression analysis of *ARR5::erGFP* in 5, 8, and 10 DAG seedlings.

Expression of *ARR5* in each background was analyzed at different time points. At 5DAG, *ARR5* was expressed in root cap and root stele of every backgrounds. There was no significant difference in *ARR5* expression between *shr-2* and *shr-2 hws-3* or *shr-2 hws-4* mutants. After 5DAG, procambium-specific expression of *ARR5* was collapsed in the rest of backgrounds (*shr-2, shr-2hws-3,* and *shr-2hws-4*). Z-section images at 5DAG shows these pattern definitely. In the mutant backgrounds (*shr-2, shr-2hws-3,* and *shr-2hws-4*), GFP signal is not expressed in the whole part of procambium but in one part. This signal also appears in the pericycle of the mutants. At 8DAG, there was still no difference between *shr* and two *shr hws* double mutants. In these, GFP signal was significantly (*shr*, *shr-2hws-3,* and *shr-2hws-4*) compared with the WT. At 10 DAG, the signal almost faded away in all the backgrounds including WT. 10 organisms were analyzed for each genotype. Scale bar(s): 50 μm (White), 20 μm (Green),10 μm (Grey). The location where Z-section was performed is indicated by the Blue line.

6. SHR regulates HWS expression in the stele

To analyze the location where *HWS* is expressed, HWS transcriptional fusion (*pHWS::erGFP*) was transformed into *shr*/+. The advantage of transforming a construct into *shr* heterozygous plants is that the expression can be compared in WT backgrounds and *shr* homozygous backgrounds without considering positional effect. The T2 generation was screened to confirm transformation. After screening, *HWS* expression analysis was performed in 5DAG seedlings. In WT backgrounds, the *HWS* was expressed in the root cap and pericycle (Gonzalez-Carranza et al., 2007) starting from the differentiation zone all the way to the boundary between hypocotyl and root (Fig. 13). In the *shr* background, *HWS* was expressed in the root cap, just like WT backgrounds. Interestingly, the GFP signal was not found in the stele of *shr* mutants (Fig. 13). This suggests that SHR activates the *HWS* in the pericycle.

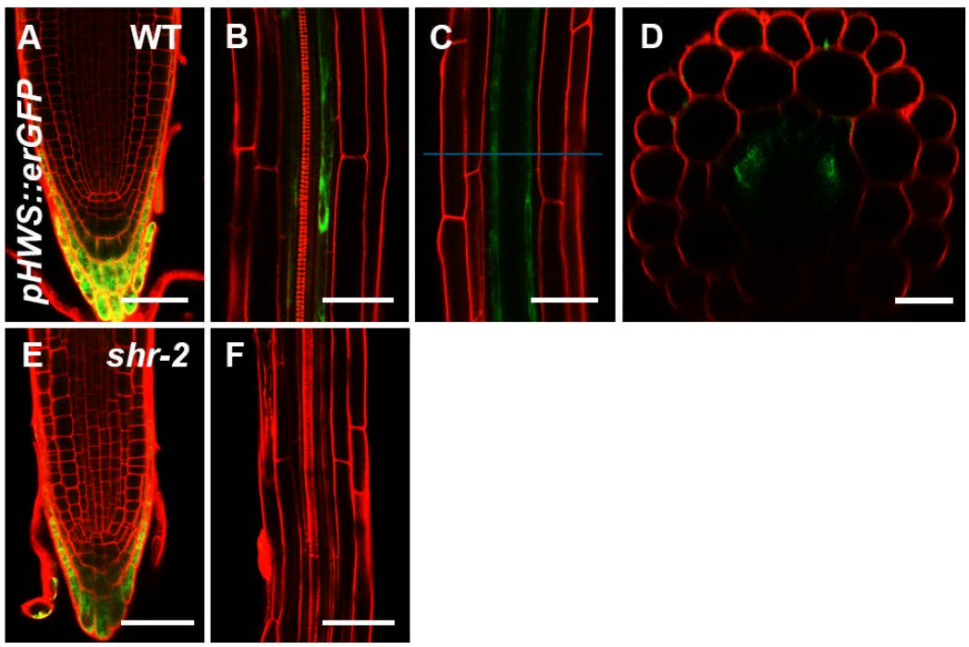

Figure 13. *HWS* expression in WT and *shr*.

HWS expression in WT (A-D) and *shr* (E, F). *HWS* is expressed in root cap of WT and *shr* (A, E). In WT, *HWS* is expressed in the stele from the starting point of xylem (B) to the bottom of the hypocotyl. To confirm the exact location where *HWS* expressed, Z-section was performed. It is expressed in the pericycle showing round GFP signal inside the stele of the root (C, D). In *shr*, there is no GFP signal in the stele (F). Blue line indicates the location where Z-section performed (C). Image was taken at 5DAG. 10 organisms were analyzed for each genotype. Scale bars: 20 μm (A, B, C, E, F), 50 μm (D)

7. Xylem patterning defect in the *shr* is not recovered in *shr-2 hws-2* and *shr-2 hws-3*.

SHR regulates xylem patterning by activating the expression of *miRNA165/6*. MiRNA165/6 which is transcriptionally activated by SHR moves towards the stele from the endodermis. HD-ZIP Ⅲ family members are expressed in the stele. MiRNA165/6 degrades the mRNAs for HD-ZIP Ⅲ family members in the stele periphery, thereby establishing the gradient of the *HD-ZIP Ⅲ* family in the stele. This action regulates xylem patterning in a dose-dependent manner. The protoxylem is formed in the stele periphery and the metaxylem in the stele center (Carlsbecker et al., 2010).

In *shr* mutants, the ectopic metaxylem develops in place of the protoxylem (Fig. 14A, adopted from Carlsbecker et al., 2010). To find wheather the xylem phenotype is affected in *shr hws*, seedlings stained in PI or fuchsin were analyzed in 5DAG and 4DAG, respectively. The metaxylem vessels usually have reticulate and pitted thickening of the secondary wall and protoxylem vessels have spiral thickening (Kubo et al., 2005). *shr hws-3* which was stained in PI didn't show the 'sprial vessels' (Fig. 14D), which indicates that protoxylem is not recovered from the *shr* phnotype. This result was consistent with the one of fuchsin staining analysis (Fig. 14E, F). *hws-2* is the T-DNA inserted knock-out mutant. The fuchsin staining data of *shr hws-2* also indicated that protoxylem is not recovered in the *shr hws* double mutant (Fig. 14B, C).

Putting these results together,there is no xylem recovery in *shr hws-2* and *shr hws-3*. This finding is consistent with the recovery of meristem acitivity in *shr hws* that is independent of the PHB-miRNA165/6 pathway.

Contrary to the result from *shr hws-2* and *shr hws-3*, PI stained *shr hws-4* roots showed protoxylem vessels (Fig. 14G). Basic fuchsin stained images of *shr hws-4* also clearly indicated the recovery of protoxylem vessels (Fig. 14I, J). This will be discribed in ‘Disscussion’.

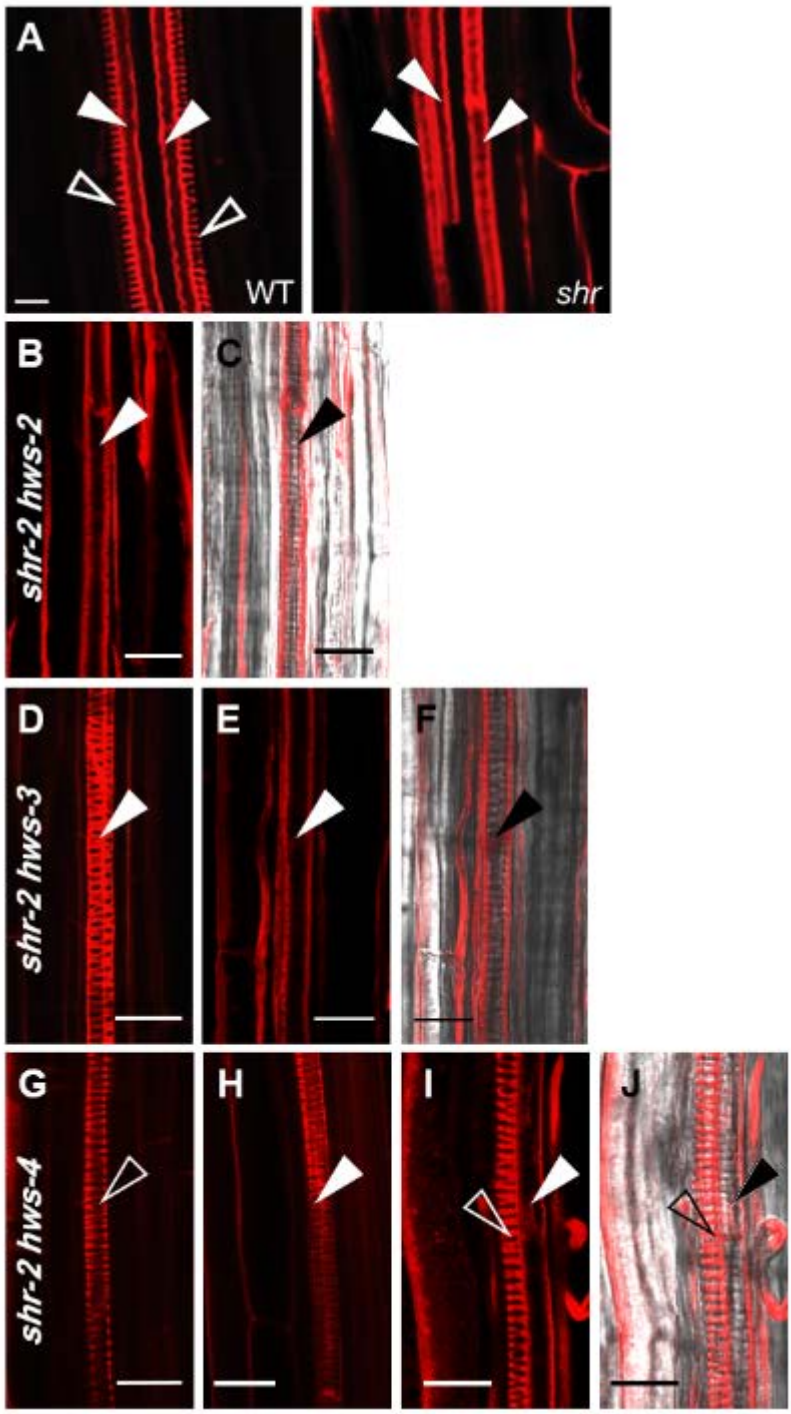
A
WT
shr
B
shr-2 hws-2
C
D
shr-2 hws-3
E
F
G
shr-2 hws-4
H
I
J

Figure 14. Xylem phenotype of *shr-2 hws-2, shr-2 hws-3,* and *shr-2 hws-4*.

(A) Confocal laser scanning micrographs of basic fuchsin-stained xylem in the root of wild type (WT) and *shr-2*. (Adopted from Carlsbecker *et al*. (2010))

In *shr* mutants, metaxylem differentiates ectopically in the place of protoxylem. Filled arrowhead indicates metaxylem, and unfilled indicates protoxylem. Scale bar: 10 μm.

(B-J) Xylem phenotype of *shr hws* mutants. Basic fuchsin staining images of *shr hws-2* (B). *shr hws-3* images of PI stained seedling (D), and fuchsin stained seedling (E). *shr hws-4* images of PI stained seedling (G, H), and fuchsin stained seedling (I). *shrhws-2* and *shrhws-3* doesn't show the protoxylem. *shrhws-4*, on the other hand, shows the restored phenotype. (C), (F), and (J) are the merged images of (B), (E), and (I), respectively, with the bright-field images. Filled arrowhead indicates metaxylem, and unfilled indicates protoxylem. Scale bars: 20 μm. Seedlings which are stained in PI was taken at 5DAG and 10 organisms were analyzed for each genotype. Seedlings which are stained in basic fuchsin was taken at 4DAG and 6 organisms were analyzed for each genotype.

Ⅳ. Discussion

1. HWS as a novel factor regulating root meristem activity in a QC-independent manner

In this study, I report the finding of HWS as a novel factor that regulates root meristem activity in a QC-independent manner. QC has been known to regulate the meristem activity (Aida et al., 2004; Sarkar et al., 2007). Recently, however, my group revealed the mechanism that regulates the root meristem activity in a QC-independent manner via PHB and B-type ARR (Sebastian et al., 2015). This led us to investigate more regulators involved in the QC-independent pathway. In *shr-2 hws-3* and *shr-2 hws-4* mutants, QC is absent but meristem cell number is as normal as WT (Figs. 8, 9, 10). Thus, *shr-2 hws-3* and *shr-2 hws-4* mutants recover meristem activity independently of QC. In *shr* mutants, a high concentration of PHB modulates B-ARR activity and suppresses root meristem activity. Thus, *TCS::erGFP* expression is restored in the stele of *shr phb* mutant, which is not expressed in the *shr* (Sebastian et al., 2015). In *shr-2 hws-3* or *shr-2 hws-4*, however, TCS expression is not restored and cytokinin signaling seems not to be the cause of meristem recovery. Thus, HWS is the novel factor regulating root meristem activity in a QC-independent manner other than the PHB-miRNA165/6-cytokinin pathway.

2. How does HWS regulate root meristem activity?

HWS is expressed in the pericycle starting from the differentiation zone and in the root cap of WT. In *shr* background, *HWS* expression disappears in the pericycle, but still exists in the root cap. This indicates that *HWS* expression is dependent on SHR in the pericycle, but it is not in the root cap. Despite the partial dependency of HWS on SHR, it seems that HWS which is expressed in the root cap is involved in the meristem activity, not in the pericycle. Because the root growth recovery is achieved in the double mutant of *SHR* and *HWS*. To confirm this, 2 different constructs were cloned, which are making *HWS* to be expressed only in the phloem pole pericycle or in the lateral root cap, respectively, and transformed into *shr hws-3*. The complemented phenotype of the transformants will tell us more clearly from which region HWS regulates the meristem activity.

Unlike the root growth phenotype, the ectopic metaxylem phenotype of *shr* is not suppressed in *shr-2 hws-2* and *shr-2 hws-3*. These results, together with the cytokinin marker expression analysis results, suggest that HWS might regulate meristem activity via a PHB-independent pathway. In *shr-2 hws-4*, however, has the protoxylem. This results seems not from the difference of the domain. *shr hws-2* is the knock out mutant and most of domains are truncated in *shr hws-3* (Fig. 4). These *shr hws-2* and *shr hws-3* have no protoxylem phenotype while *shr hws-4* does. One possible explanation is that the protoxylem formation is from another locus mutated during the EMS mutagenesis. To verify this assumption, xylem phenotype should be

analyzed in the *shr hws-4*, which is backcrossed to the wild type or other independent genotypes.

To reveal the mechanism regulating meristem activity in *shr hws*, further studies are needed. Regulation of protein stability by the ubiquitin proteasome system (UPS) includes cell division, quality control of newly produced proteins, regulation of developmental pathways, and light and phytohormone signal transduction (Ciechanover et al., 2000; Pickart, 2001; Smalle and Vierstra, 2004). Especially in the cell cycle, ubiquitination-mediated degradation of cell cycle proteins is essential. In the UPS, the target protein is conjugated with the SCF complex before degradation by 26S proteasome. Conjugation of ubiquitin to the target protein is processed by a cascade of three (E1, E2 and E3) enzymes. Among the 3 enzymes, E3 determines the substrate specificity and is considered to play the most important role in the ubiquitination reaction. SCF is one of the E3 enzyme classes and dominates cell cycle regulation. (Gusti et al., 2009). The F-box protein is the components of the SCF complex.

F-box proteins participate in lots of hormone signaling. Especially in the auxin signaling, the F-box protein, TIR1 conjugates with the AUX/IAA transcriptional repressor protein and mediates rapid degradation of AUX/IAA in the presence of auxin (Badescu and Napier, 2006; Dharmasiri et al., 2005; Kepinski and Leyser, 2005; Mockaitis and Estelle, 2008; Tan et al., 2007). Auxin is a master regulator of plant development. It mediates stem cell specification, maintenance of the root meristem, patterning and growth. Auxin concentrations promotes cell division in

roots (Overvoorde et al., 2010). Still, there are unknown mechanisms under auxin signaling. HWS is the F-box protein and cell division activity of root meristem is recovered in *shr hws*. This suggests that HWS might be a negative regulator in the auxin signaling. PIN1::PIN1:GFP (Friml et al., 2002), DR5::YFP (Friml et al., 2003), and DⅡ-VENUS (Brunoud et al., 2012) in WT backgrounds is prepared and will be crossed into *shr-2 hws-3, shr-2 hws-4*. Analysis of auxin signaling in *shr hws* will lead us to the influence of auxin signaling in this mutants.

There are lots of studies about regulation of cell cycle by SCFs. Regulation could happen either positively or negatively. In positive regulation, SCF destroys the cell cycle-dependent kinase inhibitors (CKIs) (Deshaies and Ferrell, 2001; Pagano, 2004) thus promotes the entry into S-phase. In negative regulation, SCF binds to the cell cycle regulators and prevents accumulation of those proteins (Rizzardi et al., 2015). The cell division activity will be analyzed with cell division marker, pCyclinB1.2::GUS (Donnelly et al., 1999). Furthermore, if the target protein of HWS is the cell cycle protein, target will be investigated. By employing the markers representing each phase, the phase when HWS participates will be verified. With the analyses of auxin markers and cell cycle phase markers, we could get the clues about how *shr hws* recovers meristem activities.

Ⅴ. References

Aida, M., Beis, D., Heidstra, R., Willemsen, V., Blilou, I., Galinha, C., Nussaume, L., Noh, Y.S., Amasino, R., and Scheres, B. (2004). The PLETHORA genes mediate patterning of the Arabidopsis root stem cell niche. Cell *119*, 109-120.

Austin, R.S., Vidaurre, D., Stamatiou, G., Breit, R., Provart, N.J., Bonetta, D., Zhang, J., Fung, P., Gong, Y., Wang, P.W., *et al.* (2011). Next-generation mapping of Arabidopsis genes. The Plant journal : for cell and molecular biology *67*, 715-725.

Badescu, G.O., and Napier, R.M. (2006). Receptors for auxin: will it all end in TIRs? Trends in plant science *11*, 217-223.

Bennett, T., and Scheres, B. (2010). Root development-two meristems for the price of one? Current topics in developmental biology *91*, 67-102.

Bishopp, A., Help, H., El-Showk, S., Weijers, D., Scheres, B., Friml, J., Benkova, E., Mahonen, A.P., and Helariutta, Y. (2011). A mutually inhibitory interaction between auxin and cytokinin specifies vascular pattern in roots. Current biology : CB *21*, 917-926.

Blilou, I., Xu, J., Wildwater, M., Willemsen, V., Paponov, I., Friml, J., Heidstra, R., Aida, M., Palme, K., Scheres, B. (2005). The PIN auxin efflux facilitator network controls growth and patterning in Arabidopsis roots. Nature *433*, 39-44.

Brunoud, G., Wells, D.M., Oliva, M., Larrieu, A., Mirabet, V., Burrow, A.H., Beeckman, T., Kepinski, S., Traas, J., Bennett, M.J., *et al.* (2012). A novel sensor to map auxin response and distribution at high spatio-temporal resolution. Nature *482*, 103-106.

Carlsbecker, A., Lee, J.Y., Roberts, C.J., Dettmer, J., Lehesranta, S., Zhou, J., Lindgren, O., Moreno-Risueno, M.A., Vaten, A., Thitamadee, S., *et al.* (2010). Cell signalling by microRNA165/6 directs gene dose-dependent root cell fate. Nature *465*, 316-321.

Ciechanover, A., Orian, A., and Schwartz, A.L. (2000). Ubiquitin-mediated proteolysis: biological regulation via destruction. BioEssays : news and reviews in molecular, cellular and developmental biology *22*, 442-451.

Clough, S.J., and Bent, A.F. (1998). Floral dip: a simplified method for Agrobacterium-mediated transformation of Arabidopsis thaliana. The Plant journal : for cell and molecular biology *16*, 735-743.

Cui, H., Levesque, M.P., Vernoux, T., Jung, J.W., Paquette, A.J., Gallagher, K.L., Wang, J.Y., Blilou, I., Scheres, B., and Benfey, P.N. (2007). An evolutionarily conserved mechanism delimiting SHR movement defines a single layer of endodermis in plants. Science *316*, 421-425.

Deshaies, R.J., and Ferrell, J.E., Jr. (2001). Multisite phosphorylation and the countdown to S phase. Cell *107*, 819-822.

Dharmasiri, N., Dharmasiri, S., and Estelle, M. (2005). The F-box protein TIR1 is an auxin receptor. Nature *435*, 441-445.

Di Laurenzio, L., Wysocka-Diller, J., Malamy, J.E., Pysh, L., Helariutta, Y., Freshour, G., Hahn, M.G., Feldmann, K.A., and Benfey, P.N. (1996). The SCARECROW gene regulates an asymmetric cell division that is essential for generating the radial organization of the Arabidopsis root. Cell *86*, 423-433.

Dolan, L., Janmaat, K., Willemsen, V., Linstead, P., Poethig, S., Roberts, K., and Scheres, B. (1993). Cellular organisation of the Arabidopsis thaliana root. Development *119*, 71-84.

Donnelly, P.M., Bonetta, D., Tsukaya, H., Dengler, R.E., and Dengler, N.G. (1999). Cell cycling and cell enlargement in developing leaves of Arabidopsis. Developmental biology *215*, 407-419.

Friml, J., Benkova, E., Blilou, I., Wisniewska, J., Hamann, T., Ljung, K., Woody, S., Sandberg, G., Scheres, B., Jurgens, G., *et al.* (2002). AtPIN4 mediates sink-driven auxin gradients and root patterning in Arabidopsis. Cell *108*, 661-673.

Friml, J., Vieten, A., Sauer, M., Weijers, D., Schwarz, H., Hamann, T., Offringa, R., and Jurgens, G. (2003). Efflux-dependent auxin gradients establish the apical-basal axis of Arabidopsis. Nature *426*, 147-153.

Gonzalez-Carranza, Z.H., Rompa, U., Peters, J.L., Bhatt, A.M., Wagstaff, C., Stead, A.D., and Roberts, J.A. (2007). Hawaiian skirt: an F-box gene that regulates organ fusion and growth in Arabidopsis. Plant physiology *144*, 1370-1382.

Gusti, A., Baumberger, N., Nowack, M., Pusch, S., Eisler, H., Potuschak, T., De Veylder, L., Schnittger, A., and Genschik, P. (2009). The Arabidopsis thaliana F-box protein FBL17 is essential for progression through the second mitosis during pollen development. PloS one *4*, e4780.

Haecker, A., Gross-Hardt, R., Geiges, B., Sarkar, A., Breuninger, H., Herrmann, M., and Laux, T. (2004). Expression dynamics of WOX genes mark cell fate decisions during early embryonic patterning in Arabidopsis thaliana. Development *131*, 657-668.

Helariutta, Y., Fukaki, H., Wysocka-Diller, J., Nakajima, K., Jung, J., Sena, G., Hauser, M.T., and Benfey, P.N. (2000). The SHORT-ROOT gene controls radial patterning of the Arabidopsis root through radial signaling. Cell *101*, 555-567.

Howell, S.H. (1998). Molecular Genetics of Plant Development (Cambridge University Press).

Huang, X., Feng, Q., Qian, Q., Zhao, Q., Wang, L., Wang, A., Guan, J., Fan, D., Weng, Q., Huang, T., *et al.* (2009). High-throughput genotyping by whole-genome resequencing. Genome research *19*, 1068-1076.

Kepinski, S., and Leyser, O. (2005). The Arabidopsis F-box protein TIR1 is an auxin receptor. Nature *435*, 446-451.

Koizumi, K., and Gallagher, K.L. (2013). Identification of SHRUBBY, a SHORT-ROOT and SCARECROW interacting protein that controls root growth and radial patterning. Development *140*, 1292-1300.

Kubo, M., Udagawa, M., Nishikubo, N., Horiguchi, G., Yamaguchi, M., Ito, J., Mimura, T., Fukuda, H., and Demura, T. (2005). Transcription switches for protoxylem and metaxylem vessel formation. Genes & Development *19*, 1855-1860.

Laux, T. (2003). The stem cell concept in plants: a matter of debate. Cell *113*, 281-283.

Lee, J.Y., Colinas, J., Wang, J.Y., Mace, D., Ohler, U., and Benfey, P.N. (2006). Transcriptional and posttranscriptional regulation of transcription factor expression in Arabidopsis roots. Proceedings of the National Academy of Sciences of the United States of America *103*, 6055-6060.

Lohar, D.P., Schaff, J.E., Laskey, J.G., Kieber, J.J., Bilyeu, K.D., and Bird, D.M. (2004). Cytokinins play opposite roles in lateral root formation, and nematode and Rhizobial symbioses. The Plant journal : for cell and molecular biology *38*, 203-214.

Mayer, K.F., Schoof, H., Haecker, A., Lenhard, M., Jurgens, G., and Laux, T. (1998). Role of WUSCHEL in regulating stem cell fate in the Arabidopsis shoot meristem. Cell *95*, 805-815.

Mockaitis, K., and Estelle, M. (2008). Auxin receptors and plant development: a new signaling paradigm. Annual review of cell and developmental biology *24*, 55-80.

Müller, B., and Sheen, J. (2008). Cytokinin and auxin interaction in root stem-cell specification during early embryogenesis. Nature *453*, 1094-1097.

Müller, B., and Sheen, J. (2007). Arabidopsis Cytokinin Signaling Pathway, Science *407*, cm5

Nakajima, K., Sena, G., Nawy, T., and Benfey, P.N. (2001). Intercellular movement of the putative transcription factor SHR in root patterning. Nature *413*, 307-311.

Nawy, T., Lee, J. Y., Colinas, J., Wang, J. Y., Thongrod, S. C., Malamy, J. E., Birnbaum, K., Benfey, P. N. (2005). Transcriptional profile of the Arabidopsis root quiescent center. Plant Cell *17*, 1908-1925.

Overvoorde, P., Fukaki, H., and Beeckman, T. (2010). Auxin control of root development. Cold Spring Harbor perspectives in biology *2*, a001537.

Pagano, M. (2004). Control of DNA synthesis and mitosis by the Skp2-p27-Cdk1/2 axis. Molecular cell *14*, 414-416.

Perilli, S., Sabatini, S. (2010). Analysis of root meristem size development. Methods in Molecular Biology *655*, 177-187

Pickart, C.M. (2001). Mechanisms underlying ubiquitination. Annual review of biochemistry *70*, 503-533.

Rizzardi, L.F., Coleman, K.E., Varma, D., Matson, J.P., Oh, S., and Cook, J.G. (2015). CDK1-dependent inhibition of the E3 ubiquitin ligase CRL4CDT2 ensures robust transition from S Phase to Mitosis. The Journal of biological chemistry *290*, 556-567.

Sabatini, S., Heidstra, R., Wildwater, M., and Scheres, B. (2003). SCARECROW is involved in positioning the stem cell niche in the Arabidopsis root meristem. Genes & development *17*, 354-358.

Sarkar, A.K., Luijten, M., Miyashima, S., Lenhard, M., Hashimoto, T., Nakajima, K., Scheres, B., Heidstra, R., and Laux, T. (2007). Conserved factors regulate signalling in Arabidopsis thaliana shoot and root stem cell organizers. Nature *446*, 811-814.

Scheres, B. (2007). Stem-cell niches: nursery rhymes across kingdoms. Nature reviews Molecular cell biology *8*, 345-354.

Sebastian, J., Ryu, K.H., Zhou, J., Tarkowská, D., Tarkowski, P., Cho, Y.-H., Yoo, S.-D., Kim, E.-S., and Lee, J.-Y. (2015). PHABULOSA Controls the Quiescent Center-Independent Root Meristem Activities in Arabidopsis thaliana. PLoS Genet *11*, e1004973.

Smalle, J., and Vierstra, R.D. (2004). The ubiquitin 26S proteasome proteolytic pathway. Annual review of plant biology *55*, 555-590.

Sozzani, R., and Iyer-Pascuzzi, A. (2014). Postembryonic control of root meristem growth and development. Current opinion in plant biology *17*, 7-12.

Tan, X., Calderon-Villalobos, L.I., Sharon, M., Zheng, C., Robinson, C.V., Estelle, M., and Zheng, N. (2007). Mechanism of auxin perception by the TIR1 ubiquitin ligase. Nature *446*, 640-645.

van den Berg, C., Willemsen, V., Hendriks, G., Weisbeek, P., and Scheres, B. (1997). Short-range control of cell differentiation in the Arabidopsis root meristem. Nature *390*, 287-289.

Weigel, D., and Jurgens, G. (2002). Stem cells that make stems. Nature *415*, 751-754.

Wysocka-Diller, J.W., Helariutta, Y., Fukaki, H., Malamy, J.E., and Benfey, P.N. (2000). Molecular analysis of SCARECROW function reveals a radial patterning mechanism common to root and shoot. Development *127*, 595-603.

국문초록

SHORTROOT 에 의해 조절되는 Quiescent Center 독립적인 뿌리 분열조직 활성조절 유전자 동정

Quiescent center (QC)는 뿌리 분열조직의 활성을 조절하는 것으로 알려져 있다. *SHORTROOT* knock-out 돌연변이체에서는 (*shr*), 뿌리성장과 quiescent center 유지에 결함이 있다. *SHORTROOT, PHABULOSA* double knock out 돌연변이체에서는 (*shr phb*), 뿌리 성장이 회복되지만 QC 는 회복되지 않는다. SHR 은 직접적으로 microRNA165/6 의 발현을 조절한다. microRNA165/6 는 *PHB* 와 다른 class Ⅲ HD-ZIP transcription factor 의 유전자를 분해한다. *shr* 돌연변이체에서, PHB 는 뿌리 분열조직의 중심주 안에 높은 농도로 있고, 이렇게 높은 농도로 있는 PHB 는 type B Arabidopsis Response Regulator (B-ARR)의 활성을 조절함으로써 뿌리 분열조직의 활성을 억제한다.

SHR 에 의한 뿌리성장에 관련된 새로운 인자를 찾기 위해, *shr-2* 를 ethane methyl sulfonate(EMS)로 처리하여 돌연변이시켰다. *shr-2* 뿌리보다 길게 성장한 개체가 *shr suppressors of shr (ssh)*으로서

선별되었다. 이중에서, *shr-2 ssh206* 과 *shr-2 ssh80* 이 같은 유전자인 *HAWAIIAN SKIRT* (*HWS,* AT3G61590)에 돌연변이를 갖는 것을 확인하였고, 이들을 후속 연구에 이용하였다.

shr ssh206 과 *shr ssh80* 의 뿌리길이 및 분열조직 크기는 *shr-2* 의 것보다 상당히 길지만 QC 는 완벽하게 회복되지 않는다. Allelism test 결과로, *ssh206*과 *ssh80*은 같은 *HWS* 유전자의 다른 allele 임을 알게 되었다. 따라서, *shr ssh206* 을 *shr-2 hws-3* 으로, *shr ssh80* 을 *shr-2 hws-4* 로 명명하였다.

HWS 는 root cap 과 differentiation zone 의 pericycle 에서 발현된다. *shr-2 hws-3*과 *shr-2 hws-4* 에서의 cytokinin marker 발현으로 보아, *shr hws* 분열조직 활성 회복은 cytokinin signaling 의 회복에 의한 것이 아님을 알 수 있다. 따라서, SHR 과 함께 HWS 가 뿌리 분열조직 조절에 어떻게 관여하는가를 확인하기 위해서는 후속 연구가 필요하다.

주요어 : Quiescent center, 뿌리 분열조직, SHORTROOT (SHR), HAWAIIAN SKIRT (HWS)

학 번 : 2012-20297